Case Studies in Thermal Engineering 34 (2022) 102025

Contents lists available at ScienceDirect

Case Studies in Thermal Engineering

journal homepage: www.elsevier.com/locate/csite

On the enhancement of thermal transport of Kerosene oil mixed TiO_2 and SiO_2 across Riga wedge☆

Asmat Ullah Yahya [a], Imran Siddique [b,*], Fahd Jarad [c,d,e,**], Nadeem Salamat [a], Sohaib Abdal [a,f], Y.S. Hamed [g], Khadijah M. Abualnaja [g], Sajjad Hussain [h]

[a] Department of Mathematics, Khwaja Fareed University of Engineering and Information Technology, Rahim Yar Khan, Pakistan
[b] Department of Mathematics, University of Management and Technology, Lahore, 54770, Pakistan
[c] Department of Mathematics, Cankaya University, Etimesgut, Ankara, Turkey
[d] Department of Mathematics, King Abdul Aziz University, Jeddah, Saudi Arabia
[e] Department of Medical Research, China Medical University Hospital, China Medical University, Taichung, Taiwan
[f] School of Mathematics, Northwest University, No.229 North Taibai Avenue, Xi'an, 7100069, China
[g] Department of Mathematics and Statistics, College of Science, Taif University, P. O. Box 11099, Taif, 21944, Saudi Arabia
[h] School of Aerospace and Mechanical Engineering, Nanyang Technological University, Singapore

ARTICLE INFO

Keywords:
Maxwell fluid
Heat source
Hybrid nanofluid
Riga wedge
Runge-Kutta method

ABSTRACT

Efficient thermal transportation in compact heat density gadgets is a prevailing issue to be addressed. The flow of a mono nanofluid (SiO_2/Kerosene oil) and hybrid nanofluid ($TiO_2 + SiO_2$/Kerosene oil) is studied in context of Riga wedge. The basic purpose of this work pertains to improve thermal conductivity of base liquid with inclusions of nano-entities. The hybrid nanofluid flow over Riga wedge is new aspect of this work. The concentration of new species is assumed to constitute the base liquid to be non-Newtonian. The fundamental formulation of the concentration laws of mass, momentum and energy involve partial derivatives. The associated boundary conditions are taken in to account. Similarity variables are utilized to transform the leading set of equations into ordinary differential form. Shooting procedure combined with Runge-Kutta method is harnessed to attain numerical outcomes. The computational process is run in matlab script. It is seen that the velocity component $f'(\eta)$ goes upward with exceeding inputs of modified Hartmann number Mh and it slows down when non-dimensional material parameter α_h takes large values. Also, Nusselt number $-\theta'(0)$ is enhanced with developing values of Eckert number Ec and Biot number B_i.

Nomenclature

Latin Symbols

u, v	Velocity components
x, y	Cartesian coordinates
K	permeability

☆ Fully documented templates are available in the elsarticle package on CTAN.

* Corresponding author.
** Corresponding author. Department of Mathematics, Cankaya University, Etimesgut, Ankara, Turkey.
E-mail addresses: imransmsrazi@gmail.com (I. Siddique), fahd@cankaya.edu.tr (F. Jarad).

https://doi.org/10.1016/j.csite.2022.102025
Received 4 December 2021; Received in revised form 20 March 2022; Accepted 6 April 2022
Available online 14 April 2022

k^*	permeability of porous medium
j_0	current density of electrodes
K_{hnf}	hybrid nanofluid thermal conductivity
M_0	permanent magnetized magnate
d	width between the electrodes
Q_0	heat source coefficient
Q	heat source
T	Temperature
E_c	Eckert number
T_∞	Ambient fluid temperature
M_h	Hartmann number
α_h	dimensionless parameter
Pr	Prandtl number
T_w	Wall temperature
Re_x	Reynolds number
h_f	heat transfer coefficient

Greek Symbols

α_h	dimensionless parameter
ρC_p	heat capacity
μ_{hnf}	fluid dynamic velocity
ρ_{hnf}	density of hybrid nanofluid
ν	Kinematic viscosity
μ	Fluid viscosity
β	wedge angle parameter
ρ	Fluid density
λ	Deborah number
λ_1	relaxation time
η	Similarity variable
σ	electrical conductivity

Subscripts

p	Nanoparticles
w	On the wall
∞	Ambient

1. Introduction

All those fluids which can't be fulfill the Newton's law of viscosity are known as Non-Newtonian fluids. Common examples of non-Newtonian fluids are dissolved margarine, ketchup, squeezed apple, corn starch, starch suspensions and cleanser etc. A well known Non-Newtonian fluid is Maxwell fluid. Jamshed et al. [1] investigated the impacts of MHD Maxwell nanofluids. Abdal et al. [2] studied bioconvection of living microorganisms on MHD Maxwell nanofluid flow. Habib et al. [3] studied the comparative study of different non-Newtonian fluids. The impacts of chemical reaction on Maxwell nanofluid flow through a permeable surface with radiation was depicted by Ali et al. [4]. Bilal et al. [5] analyzed the radiative heat flux effect for Maxwell nanofluid flow in three dimension. Abdal et al. [6] discussed PST and PHF condition on MHD Maxwell nanofluid with living microorganisms. Similar work were done by [7–9].

In the recent last few decades various experts explored the progress in the thermal conductivity. Nano-fluid constituted of colloidal suspension of nanometer shaped particles in base liquid. These nano-fluids are favorable for the growth of thermal transportation to be known for microelectronics, refrigeration and cooling, sun collected heat, compact and processors of Personal computers etc. Inherently, the up-gradation of heat transportation based on the thermal conductivity of nano-particles, fixations of volume atom and mass stream rates. Initially, Choi [10] analyzed the heat transfer of nanofluids. The effect of nanofluids in a photovoltaic systems and solar plates collectors was depicted by Sheikholeslami et al. [11]. Yang et al. [12] analyzed the heat coefficient in bone micro grinding for using nanofluid aerosol cooling. The investigation of nanofluid flow through a Riga plate with heated bio-convection process was studied by Bhatti et al. [13]. Rostami et al. [14] examined the measurement of heat flow of MWCNT-CuO/water nanofluid by using artificial neural networks (ANNs). By using the silver-water nanofluid in three dimensions hemispherical of solar collector operating was depicted by Moravej et al. [15]. Similar work were done by many mathematicians [16–19].

To improve the efficiency of transfer of heat of nanoparticles, the researchers are planning to dope more than one specie the nanoparticles called hybrid nanoparticles. Such types of particles are obtained by adding at least two unlike materials nano-sized particles. These fluids are utilized in different fields like cooling vehicles motor, electronic cooling, machine coolant and so forth. Toghraie et al. [20] studied the viscosity of nanofluid (Silver/Ethylene glycol) at various volume fractions and temperature of

nano-particles and design an artificial neural network (ANN), similar work was presented in Refs. [21,22]. The investigation of single and hybrid base nanofluids with WO_3 and MWCNTs to enhance the thermal conductivity of fluids was analyzed by Soltani et al. [23]. Ruhani et al. [24] explored the statistical investigation for the enhancement of a new mathematical model for rheological behavior of Silica-ethylene glycol/water hybrid Newtonian nanofluid. Khodabandeh et al. [25] studied the improvement in thermal conductivity of water nanofluid/GNP-SDBS in double-layer micro-channel heat sink with sinusoidal cavities. Yan et al. [26] depicted the rheological behavior of MWCNTs-ZnO/water-ethylene glycol hybrid non-Newtonian nanofluid by using an experimental investigation. Abro et al. [27] experimental investigated mild steel. Alarifi et al. [28] analytically performed the quality assurance of impact-damaged laminate composite structures. further, Asmatulu et al. [29] investigated the effects of surface treatments on carbon fiber-reinforced composite laminates. Many researchers were done similar work on nanofluid [30–35].

Heat source is usually used to increase the heat of the objects. Radiation impacts on hybrid nanofluid (Fe_3O_4/*graphene*) flow through a folded sheet with heat source was analyzed by Acharya et al. [36]. Tlili et al. [37] investigated the impacts of heat resistive flow on MHD Sakiadis hybrid nanofluid transportation through thin needle. Analysis of heat conductivity of hybrid nanofluid Cu–Al_2O_3 with viscous dissipation was investigated by Aamir et al. [38]. Chamkha et al. [39] discussed presence of heat source in square shaped flow of hybrid nanofluid with MHD free convection. Evaluation of exact solution of Stokes second theorem with the flow of hybrid nanofluid was examined by Roy et al. [40]. Shehzad et al. [41] examined the conduction of heat in radiative hybrid nanofluid through a permeable domain. The increase in heat transfer rate in hybrid nanofluid with micro heat exchanger and its computational investigation was studied by Ghachem et al. [42].

From the survey of above related literature on the improvement of heat transfer in fluids, various techniques such as fin and fan increase the size of the heat exchanger. However, the concept of increased thermal conductivity of base fluid with the inclusion of nano-entities has become very popular. This work presents enhancement in thermal transportation of Kerosene oil slightly mixed with nano particles of SiO_2 and ($SiO_2 + TiO_2$). The nanofluid transportation occurs across Riga wedge. This is novel aspect of this work to consider thermal transportation of two types of nanofluids (mono nanofluid and hybrid nanofluid) across Riga wedge. This work is rarely discussed in the existing literature. The very interest for this communication aroused to reduce thermal imbalances arising in concurrent complicated technological procedures pertaining to industries, transportation and electronics.

2. Mathematical formulation

We consider the fluid flow is incompressible, independent of time and two dimensional. On a Riga wedge surface a simple nanofluid SiO_2/Kerosene oil and hybrid nanofluid $TiO_2 + SiO_2$/Kerosene oil flow pattern are shown in Fig. 1. Suppose that the Riga wedge surface is taken along the direction of $x - axis$ and $y - axis$ is drawn perpendicular to it. The velocity of fluid is denoted by u and v, which are taken along the x and $y - axis$ respectively, fluid dynamic viscosity is named as μ_{hnf}, T is temperature, k^* is the permeability of porous medium, J_0 is expressing the current density of electrodes, density of hybrid nanofluid is denoted by ρ_{hnf}, k_{hnf} is the hybrid nanofluid thermal conductivity, permanent magnetized magnate is named as M_0, width between the electrodes is labeled as d, Q_0 is the coefficient of heat source/sink, heat capacity of fluid is named as $\rho\ C_p$, λ_1 is relaxation time. The wedge surface is stretched with a velocity $U_w = u_w x^m$ and $U_e = u_e x^m$ is labeled as free stream velocity, an ambient temperature of fluid is denoted as T_∞, heat transfer coefficient is labeled as h_f and wall temperature is named as T_w. Thermo-physical characteristics are presented in Table 1. Here, we take the percentage volume for nano-particles SiO_2/Kerosene oil is 0.01 in bulk of TiO_2/Kerosene oil. In this problem $\varphi_1 = 0.04$ and $\varphi_2 = 0$ for TiO_2/Kerosene oil. For hybrid nanofluid, volume-fraction $\varphi_1 = 0.03$ (TiO_2) and $\varphi_2 = 0.01$ (SiO_2) is assumed. For hybrid nano-fluid and nanofluid the thermo-physical characteristics are disclosed in Table 2.

With the above assumption the flow model is [35,43,44]

$$\frac{\partial u}{\partial x} + \frac{\partial v}{\partial y} = 0, \tag{1}$$

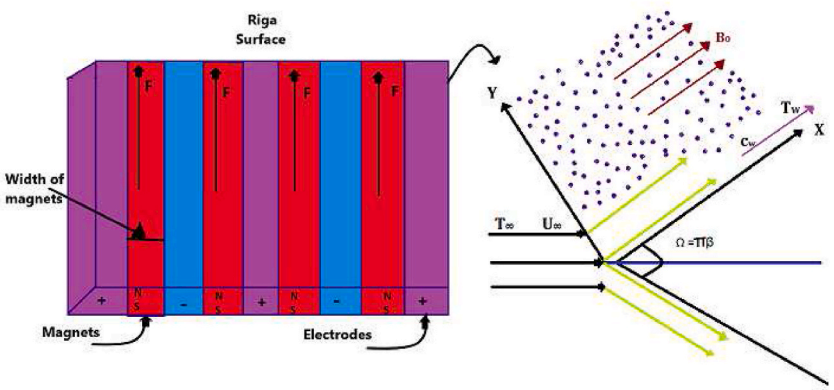

Fig. 1. Flowchart.

Table 1
Thermo-physical properties [45,46].

Physical properties	TiO_2	SiO_2	Kerosene oil
$\rho(kg.m^{-3})$	4230	2220	783
$C_p(J(kg.^{\circ}k$	692	745	2090
$\kappa(W(m.^{\circ}k)$	8.4	1.4	0.145

Table 2
Thermal characteristics [14,23,35,43].

Properties	Nanofluid	Hybrid Nanofluid
μ(viscosity)	$\mu_{nf} = \frac{\mu_f}{(1-\Phi)^{2.5}}$	$\mu_{hnf} = [\frac{\mu_f}{(1-\Phi_1)^{2.5}(1-\Phi_2)^{2.5}}]$
ρ(density)	$\rho_{nf} = \rho_f((1-\Phi) + \Phi\frac{\rho_s}{\rho_f}$	$\rho_{hnf} = [\rho_f(1-\Phi_2)((1-\Phi_1) + \Phi_1\frac{\rho_{s1}}{\rho_f}) + \Phi_2\rho_{s2}]$
ρC_p(Heat capacity)	$(\rho C_p)nf = (\rho C_p)_f((1-\Phi) + \Phi\frac{(\rho C_p)_s}{(\rho C_p)_f}$	$(\rho C_p)_{hnf} = [(\rho C_p)_f(1-\Phi_2)((1-\Phi_1) + \Phi_1\frac{(\rho C_p)_{s1}}{(\rho C_p)_f}) + \Phi_2(\rho C_p)_{s2}]$
κ(Thermal conductivity)	$\frac{\kappa_{nf}}{\kappa_f} = \frac{\kappa_s + (s_f-1)\kappa_f - (s_f-1)\Phi(\kappa_f-\kappa_s)}{\kappa_s + (s_f-1)\kappa_f + \Phi(\kappa_f-\kappa_s)}$	$\frac{\kappa_{hnf}}{\kappa_{bf}} = [\frac{\kappa_{s2} + (s_f-1)\kappa_{bf} - (s_f-1)\Phi_2(\kappa_{bf}-\kappa_{s2})}{\kappa_{s2} + (s_f-1)\kappa_{bf} + \Phi(\kappa_{bf}-\kappa_{s2})}]$ where $\frac{\kappa_{bf}}{\kappa_f} = [\frac{\kappa_{s1} + (s_f-1)\kappa_f - (s_f-1)\Phi_1(\kappa_f-\kappa_{s1})}{\kappa_{s1} + (s_f-1)\kappa_f + \Phi(\kappa_f-\kappa_{s1})}]$
σ(Electrical conductivity)	$\frac{\sigma_{nf}}{\sigma_f} = 1 + \frac{3(\sigma-1)\Phi}{(\sigma+2) - (\sigma-1)\Phi}$	$\frac{\sigma_{hnf}}{\sigma_{bf}} = [1 + \frac{3\Phi(\sigma_1\Phi_1 + \sigma_2\Phi_2 - \sigma_{bf}(\Phi_1+\Phi_2))}{(\sigma_1\Phi_1 + \sigma_2\Phi_2 + 2\Phi\sigma_{bf}) - \Phi\sigma_{bf}((\sigma_1\Phi_1 + \sigma_2\Phi_2) - \sigma_{bf}(\Phi_1+\Phi_2))}]$

$$u\frac{\partial u}{\partial x} + v\frac{\partial u}{\partial y} = \frac{\mu_{hnf}}{\rho_{hnf}}\frac{\partial^2 u}{\partial y^2} + \frac{J_0 M_0 \pi}{8} exp\left(-\frac{\pi}{d}y\right) - \frac{\mu_{hnf}}{\rho_{hnf}}\frac{u}{k^*} + \lambda_1\left(u^2\frac{\partial^2 u}{\partial x^2} + v^2\frac{\partial^2 u}{\partial y^2} + 2uvu^2\frac{\partial^2 u}{\partial y \partial x}\right), \tag{2}$$

$$u\frac{\partial T}{\partial x} + v\frac{\partial T}{\partial y} = \frac{k_{hnf}}{(\rho C_p)_{hnf}}\frac{\partial^2 T}{\partial y^2} + \frac{\mu_{hnf}}{(\rho C_p)_{hnf}}\left(\frac{\partial u}{\partial x}\right)^2 + \frac{Q_0}{(\rho C_p)_{hnf}}(T - T_\infty). \tag{3}$$

With supportive boundary condition [35]:

$$\left.\begin{aligned} u = U_w = cx, v = 0, -k_{hnf}\frac{\partial T}{\partial y} = h_f(T - T_w), \ as\ y = 0, \\ u \to u_e, \ T \to T_\infty, \ as\ y \to \infty. \end{aligned}\right\} \tag{4}$$

Physical properties of Kerosene oil are given in Table 2.
The transformed ordinary differential equations are:

$$\begin{aligned} &f''' - A_1\left(\frac{2m}{m+1}f'^2 - ff''\right) - A_1\frac{2}{m+1}Mh(\alpha_h\eta) - K_pAf' \\ &+A_1\beta_{max}\left(\frac{2m(m-1)}{m+1}f'^3 + \frac{(m-1)^3}{m+1}\eta f'^2 f''' + \frac{m-1}{2m+2}\eta^2 f'^2 f''' + (m+1)f^2 f''' - ff'f'''\right) = 0, \end{aligned} \tag{5}$$

$$\theta'' - \frac{k_f}{k_{hnf}}Pr\left(A_3 f\theta' - EcA_4 f'^2 - \frac{2}{m+1}Q\theta\right) = 0, \tag{6}$$

$$\left.\begin{aligned} f(\eta) = 0, \ f'(\eta) = 1, \ \frac{k_{hnf}}{k_f}\theta'(\eta) = B_i(1-\theta(\eta)), \ at\ \eta = 0, \\ f'(\infty) \to 1, \ \theta(\infty) \to 0, \ as\ \eta \to \infty. \end{aligned}\right\} \tag{7}$$

where, $M_h = \frac{\pi J_0 M_0}{8a^2 x^{2m-1}}$, $\alpha_h = (\frac{2\nu}{a(m+1)x^{m-1}})^{1/2}\frac{\pi}{d}$, $K_p = \frac{\mu}{k^*}$, $\beta = \frac{2m}{m+1}$, $Q = \frac{2Q_0}{a(\rho C_p)_{hnf}(m+1)x^{m+1}}$, $Ec = \frac{a^2x^{2m}}{(C_p)_f(T_w - T_\infty)}$, $Pr = \frac{\nu_f(\rho C_p)_f}{\kappa_f}$ and $\lambda = \lambda_1 a x^{m-1}$ are modified Hartmann number, dimensionless parameter, porosity parameter, wedge angle parameter, heat source parameter, Eckert number, Prandtl number and Deborah number. Also

$$A_1 = \left[(1-\Phi_1)^{2.5}(1-\Phi_2)^{2.5}\left[\left(1-\Phi_2\right)\left\{\left(1-\Phi_1\right)+\Phi_1\frac{\rho_{s1}}{\rho_f}\right\}+\Phi_2\frac{\rho_{s2}}{\rho_f}\right]\right.,$$

$$A_2 = \left[\left(1-\Phi_2\right)\left\{\left(1-\Phi_1\right)+\Phi_1\frac{\rho_{s1}}{\rho_f}\right\}+\Phi_2\frac{\rho_{s2}}{\rho_f}\right],$$

$$A_3 = \left[\left(1-\Phi_2\right)\left\{\left(1-\Phi_1\right)+\Phi_1\frac{(\rho C_p)_{s1}}{(\rho C_p)_f}\right\}+\Phi_2\frac{(\rho C_p)_{s2}}{(\rho C_p)_f}\right],$$

$$A_4 = [(1-\Phi_1)^{2.5}(1-\Phi_2)^{2.5}],$$

$$\frac{k_{hnf}}{k_f} = \left[\frac{\kappa_{s2}+(s_f-1)\kappa_{bf}-(s_f-1)\Phi_2(\kappa_{bf}-\kappa_{s2})}{\kappa_{s2}+(s_f-1)\kappa_{bf}+\Phi_2(\kappa_{bf}-\kappa_{s2})}.\frac{\kappa_{s1}+(s_f-1)\kappa_f-(s_f-1)\Phi_1(\kappa_f-\kappa_{s1})}{\kappa_{s1}+(s_f-1)\kappa_f+\Phi_1(\kappa_f-\kappa_{s1})}\right].$$

Physical quantities are (see Ref. [35]):

$$C_f=\frac{\tau_w}{\rho_f U_w^2},\ Nu=\frac{xq_w}{k_f(T_w-T_\infty)},\ \tau_w=\mu_{hnf}(1+\lambda_1)\left(\frac{\partial u}{\partial y}\right),\ q_w=k_{hnf}\frac{\partial T}{\partial y},\ at\ y=0, \tag{8}$$

Using similarity transformation, we get

$$\begin{cases} Cf_x Re_x^{1/2}=\dfrac{(1+\lambda)f''(0)}{A_4}, \\ Nu_x Re_x^{-1/2}=-\dfrac{\left[k_{hnf}\theta'(0)\right]}{k_f}.ed \end{cases}$$

3. Solution procedure

The non-linear boundary value problems constituted by eq. (5) to eq. (7) is difficult to solve analytically. A numerical procedure involving Runge-Kutta method is coded in matlab script. The higher order derivatives are reduced to a system of first order differential equations as given below:

$s_1' = s_2$

$s_2' = s_3$

$(1+WeA_1s_3)s_3' = A_1(s_2^2 - s_1s_3) + A_2Ms_2 + K_ps_2$

$s_3' - A_1\left(\frac{2m}{m+1}s_2^2 - s_1s_3\right) - A_1\frac{2}{m+1}Mhexp(-\frac{\pi}{d}\eta) - KAs_2 + A_1\beta_m ax\left(\frac{2m(m-1)}{m+1}s_2^3 + \frac{(m-1)^3}{m+1}\eta s_2^2 + \frac{m-1}{2m+2}\eta^2 s_2^2 s_3' + (m+1)s_1^2 s_3' - s_1 s_2 s_3'\right) = 0,$

$s_4' = s_5$

$s_5' = \frac{k_f}{k_{hnf}}Pr(A_3s_1s_5 - EcA_4s_3^2 - Qs_4)$

Along with the boundary conditions:

$s_1 = 0,\ s_2 = 1,\ s_4 = 1,\ \text{at}\ \eta = 0$

$s_2 \to 0,\ s_4 \to 0\ as\ \eta \to \infty.$

4. Outcomes and discussion

Here, two cases of fluid flow are computed and expressed for their numerical solution. First case is SiO_2/Kerosene oil and second case is $TiO_2 + SiO_2$/Kerosene oil. The four sets of results are contained in Table 3 and a close co-relation is seen among all of them. The numerical findings for the dependent physical quantities are yielded by utilizing Runge-Kutta procedure. This method is widely used for solution of such problems. This is efficient and straight method with accuracy $O(h^5)$. Reliability of the numerical scheme is ascertained in limiting cases as enlisted in Table 3. A good comparison is seen among previous and current findings. Computations are prepared to elucidate the thermal and mass transfer by Maxwell hybrid nanofluid when the dimensionless numbers of influence are varied in appropriate ranges.

In each of Figs. 2–5, results for SiO_2/Kerosene oil and for $TiO_2 + SiO_2$/Kerosene oil are presented. The fixed Prandtl number $Pr = 30$ is taken. Fig. 2 depicts the influence of modified Hartmann number Mh and dimensionless parameter α_h on $f'(\eta)$. It comes to know that for both nanofluids, velocity goes upward with large Mh and it slows down when α_h takes large values. The modified Hartmann number Mh is related to the design of Riga surface which reduce the friction to the flow and hence acceleration is resulted. Fig. 3, delineated to

Table 3
Comparative outputs of $-\theta'(0)$.

Pr	Wang [47]	Khan and Pop [48]	Yahya et al. [43]	Our results
2.0	0.9114	0.9113	0.9112	0.9114
6.13	–	–	1.7597	1.7595
7.0	1.8954	1.8954	1.8953	1.8954
20.0	3.3539	3.3539	3.3540	3.3540

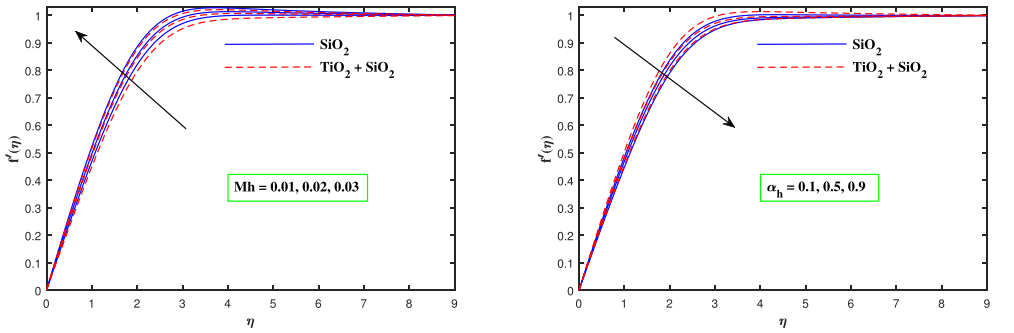

Fig. 2. The curve for velocity $f'(\eta)$ with fluctuation of Mh and α_h.

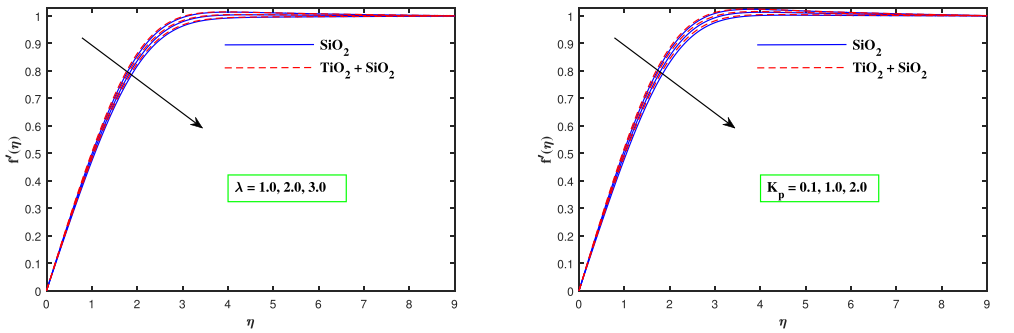

Fig. 3. The curve for velocity $f'(\eta)$ with fluctuation of λ and K_p.

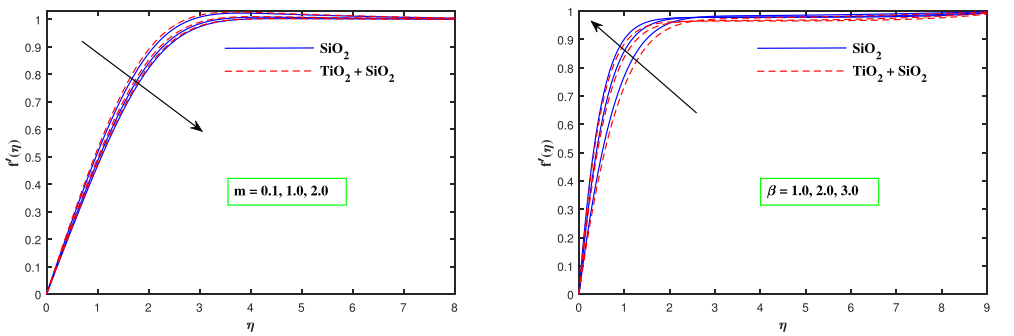

Fig. 4. The curve for velocity $f'(\eta)$ with fluctuation of m and β.

capture impact of λ and Kp, the porosity parameter on $f'(\eta)$. The flow decelerates against (λ and Kp). The main reason behind the decreases in velocity is that λ, the Debora number is related with relaxation time due to this large value of λ, the velocity declines. Also, there exists higher resistance the flow when Kp intensifies so, velocity decreases. Fig. 4, demonstrates the inputs of nonlinear parameter m and wedge angle β, on velocity $f'(\eta)$. The velocity recedes down against the parameter m but it increases more rapidly with the rising values of β. The very reason behind this inclination is that the higher wedge angle slows the motion of fluid which causes decrease in boundary layer thickness. The variation of temperature for the simple and hybrid nanofluids for different values of Ec and Q is demonstrated in Fig. 5. It is seen that when Ec increases, temperature goes down for both fluids. The basic reason behind this retardation is that the larger values of Ec convert the mechanical energy to heat energy. On the other hand, temperature increases for both fluids with the rising values of Q. Physically, more additional heat provided to the liquid when heat source takes larger values which enhances the temperature of the fluid. In Fig. 5, the impact of volume fraction φ_2 and B_i is observed. It is seen that with the enhancement in values of φ_2, temperature rises. The basic reason behind this phenomenon is that the thermal conductivity rises with the increasing values of φ_2. Similarly, temperature increases for Biot number for both the fluids. Physically, there is direct relation between Biot number and temperature. So, temperature rises rapidly with increasing values of B_i. Moreover, for the different inputs of

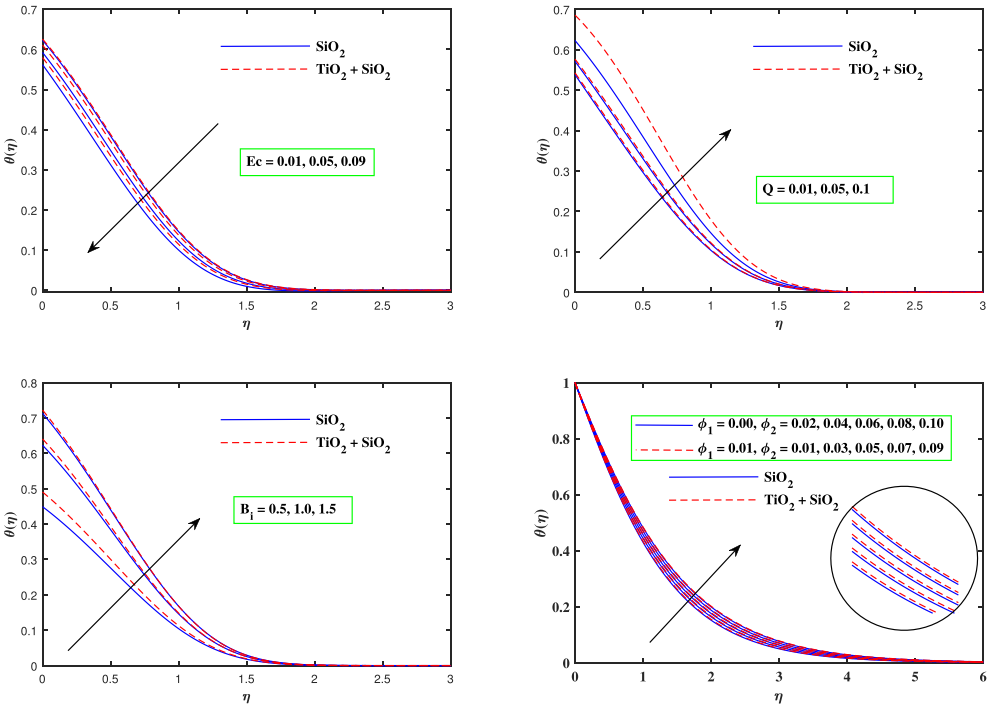

Fig. 5. The curve for temperature $\theta(\eta)$ with fluctuation of Ec, Q, B_i and φ_2.

the numbers λ, K_p, Mh, m and α_h the outputs of skin friction $-f''(0)$ are enlisted in Table 4. It is observed that absolute values of $-f''(0)$ is enhanced with Mh and λ. However, $-f''(0)$ diminishes when the parameter λ, Kp, m and α_h are incremented. Also, Nusselt number $-\theta'(0)$ is enhanced with developing values of Ec and B_i as detailed in Table 5. It is noticed that $-\theta'(0)$ diminishes against heat source parameter Q.

5. Conclusions

In order to enhance flow thermal transportation, mono nanofluid (SiO_2/Kerosene oil) and hybrid nanofluid ($TiO_2 + SiO_2$/Kerosene oil) is discussed across a Riga wedge. Theoretical and numerical investigation is made and that findings are attained for the two cases. The valuable findings are summarizes as below:

- When the dimensionless parameters α_h, K_p, λ and m increase, the velocity decreases while opposite behavior is noticed for Mh and β.
- With the rising values of Ec, temperature goes down while the temperature is boosted up with Q and B_i.
- With the growing value of φ_2, the temperature $\theta(\eta)$ is uplifted.
- The coefficient of skin friction factor rises with M_h and λ but the growing values of m, K_p and α_h causes to reduce the magnitude of $-f''(0)$.
- With developing values of Ec and B_i, progressive behavior is shown for Nusselt number $-\theta'(0)$ but it is inversely proportional to Q.
- It is perceived that temperature distribution and heat transfer is increased in case of hybrid nanofluid.

6. Future direction

In future this problem can be extended for bioconvection of living microorganisms and with different numerical techniques like FEM, FDM and Artificial neural network ([20,22]).

Funding

Not applicable.

CRediT author statement

Conceptualization; Imran Siddique, Sohaib Abdal and Fahd Jarad. Methodology; Imran Siddique, Sajjad Hussain and Y. S. Hamed. Formal analysis: Y. S. Hamed. Funding acquisition; Fahd Jarad, Y. S. Hamed and Khadijah M. Abualnaja. Investigation; Nadeem Salamat. Writing—original draft preparation; Asmat Ullah Yahya and Sohaib Abdal. Software; Sohaib Abdal and Asmat Ullah Yahya. Validation; Y. S. Hamed. Writing—review and editing; Imran Siddique, Sajjad Hussain and Khadijah M. Abualnaja. Supervision; Imran

Table 4
Results for Skin friction factor $-f''(0)$.

m	Mh	λ	K_p	α_h	SiO_2	$TiO_2 + SiO_2$
0.5	0.02	0.2	1.0	0.01	0.6952	0.7044
1.0					0.6742	0.6829
1.5					0.6621	0.6707
0.5	0.01				0.6491	0.6575
	0.02				0.6952	0.7044
	0.03				0.7402	0.7501
	0.02	0.1			0.6381	0.6465
		0.2			0.6952	0.7044
		0.3			0.7522	0.7621
		0.2	0.5		0.7077	0.7167
			1.0		0.6952	0.7044
			1.5		0.6829	0.6921
			1.0	0.01	0.6952	0.7044
				0.02	0.6930	0.7021
				0.03	0.6908	0.6999

Table 5
Results for Nusselt number $-\theta'(0)$.

Q	Ec	B_i	SiO_2	$TiO_2 + SiO_2$
0.01	0.01	1.0	0.4889	0.4882
0.05			0.4540	0.4542
0.1			0.3994	0.4011
	0.01		0.3994	0.4011
	0.02		0.4075	0.4092
	0.03		0.4155	0.4173
	0.01	0.5	0.2916	0.2919
		1.0	0.3994	0.4011
		1.5	0.4556	0.4583

Siddique and Sajjad Hussain. All authors have read and agreed to the published version of the manuscript.

Declaration of competing interest

The authors declare that they have no known competing financial interests or personal relationships that could have appeared to influence the work reported in this paper.

Availability of data and materials

Not applicable.

Acknowledgement

This Research was supported by Taif University Researchers Supporting Project Number (TURSP-2020/217), Taif University, Taif, Saudi Arabia.

References

[1] W. Jamshed, Numerical investigation of mhd impact on maxwell nanofluid, Int. Commun. Heat Mass Tran. 120 (2021), 104973.
[2] S. Abdal, I. Siddique, D. Alrowaili, Q. Al-Mdallal, S. Hussain, Exploring the magnetohydrodynamic stretched flow of williamson maxwell nanofluid through porous matrix over a permeated sheet with bioconvection and activation energy, Sci. Rep. 12 (1) (2022) 1–12.
[3] U. Habib, S. Abdal, I. Siddique, R. Ali, A comparative study on micropolar, williamson, maxwell nanofluids flow due to a stretching surface in the presence of bioconvection, double diffusion and activation energy, Int. Commun. Heat Mass Tran. 127 (2021), 105551.
[4] B. Ali, Y. Nie, S.A. Khan, M.T. Sadiq, M. Tariq, Finite element simulation of multiple slip effects on mhd unsteady maxwell nanofluid flow over a permeable stretching sheet with radiation and thermo-diffusion in the presence of chemical reaction, Processes 7 (9) (2019) 628.
[5] M. Bilal, M. Sagheer, S. Hussain, Three dimensional mhd upper-convected maxwell nanofluid flow with nonlinear radiative heat flux, Alex. Eng. J. 57 (3) (2018) 1917–1925.
[6] S. Abdal, I. Siddique, S. Afzal, Y.-M. Chu, A. Ahmadian, S. Salahshour, On development of heat transportation through bioconvection of maxwell nanofluid flow due to an extendable sheet with radiative heat flux and prescribed surface temperature and prescribed heat flux conditions, Math. Methods Appl. Sci. (2021), https://doi.org/10.1002/mma.7722.
[7] S. Abdal, U. Habib, I. Siddique, A. Akgül, B. Ali, Attribution of multi-slips and bioconvection for micropolar nanofluids transpiration through porous medium over an extending sheet with pst and phf conditions, Int. J. Algorithm. Comput. Math. 7 (6) (2021) 1–21.
[8] S. Abdal, I. Siddique, A.S. Alshomrani, F. Jarad, I.S.U. Din, S. Afzal, Significance of chemical reaction with activation energy for riga wedge flow of tangent hyperbolic nanofluid in existence of heat source, Case Stud. Therm. Eng. 28 (2021), 101542.
[9] S. Afzal, I. Siddique, F. Jarad, R. Ali, S. Abdal, S. Hussain, Significance of double diffusion for unsteady carreau micropolar nanofluid transportation across an extending sheet with thermo-radiation and uniform heat source, Case Stud. Therm. Eng. 28 (2021), 101397.

[10] S.U. Choi, J.A. Eastman, Enhancing Thermal Conductivity of Fluids with Nanoparticles, Tech. rep., Argonne National Lab., IL (United States), 1995.
[11] M. Sheikholeslami, S.A. Farshad, Z. Ebrahimpour, Z. Said, Recent progress on flat plate solar collectors and photovoltaic systems in the presence of nanofluid: a review, J. Clean. Prod. (2021), 126119.
[12] M. Yang, C. Li, L. Luo, R. Li, Y. Long, Predictive model of convective heat transfer coefficient in bone micro-grinding using nanofluid aerosol cooling, Int. Commun. Heat Mass Tran. 125 (2021), 105317.
[13] M. Bhatti, E.E. Michaelides, Study of arrhenius activation energy on the thermo-bioconvection nanofluid flow over a riga plate, J. Therm. Anal. Calorim. 143 (3) (2021) 2029–2038.
[14] S. Rostami, D. Toghraie, B. Shabani, N. Sina, P. Barnoon, Measurement of the thermal conductivity of mwcnt-cuo/water hybrid nanofluid using artificial neural networks (anns), J. Therm. Anal. Calorim. 143 (2) (2021) 1097–1105.
[15] M. Moravej, M.H. Doranehgard, A. Razeghizadeh, F. Namdarnia, N. Karimi, L.K. Li, H. Mozafari, Z. Ebrahimi, Experimental study of a hemispherical three-dimensional solar collector operating with silver-water nanofluid, Sustain. Energy Technol. Assessments 44 (2021), 101043.
[16] Z. Li, P. Barnoon, D. Toghraie, R.B. Dehkordi, M. Afrand, Mixed convection of non-Newtonian nanofluid in an h-shaped cavity with cooler and heater cylinders filled by a porous material: two phase approach, Adv. Powder Technol. 30 (11) (2019) 2666–2685.
[17] A.R. Rahmati, O.A. Akbari, A. Marzban, D. Toghraie, R. Karimi, F. Pourfattah, Simultaneous investigations the effects of non-Newtonian nanofluid flow in different volume fractions of solid nanoparticles with slip and no-slip boundary conditions, Therm. Sci. Eng. Prog. 5 (2018) 263–277.
[18] W. He, D. Toghraie, A. Lotfipour, F. Pourfattah, A. Karimipour, M. Afrand, Effect of twisted-tape inserts and nanofluid on flow field and heat transfer characteristics in a tube, Int. Commun. Heat Mass Tran. 110 (2020), 104440.
[19] P. Barnoon, D. Toghraie, F. Eslami, B. Mehmandoust, Entropy generation analysis of different nanofluid flows in the space between two concentric horizontal pipes in the presence of magnetic field: single-phase and two-phase approaches, Comput. Math. Appl. 77 (3) (2019) 662–692.
[20] D. Toghraie, N. Sina, N.A. Jolfaei, M. Hajian, M. Afrand, Designing an artificial neural network (ann) to predict the viscosity of silver/ethylene glycol nanofluid at different temperatures and volume fraction of nanoparticles, Phys. Stat. Mech. Appl. 534 (2019), 122142.
[21] W. He, B. Ruhani, D. Toghraie, N. Izadpanahi, N.N. Esfahani, A. Karimipour, M. Afrand, Using of artificial neural networks (anns) to predict the thermal conductivity of zinc oxide–silver (50%–50%)/water hybrid Newtonian nanofluid, Int. Commun. Heat Mass Tran. 116 (2020), 104645.
[22] S. Rostami, D. Toghraie, M.A. Esfahani, M. Hekmatifar, N. Sina, Predict the thermal conductivity of sio2/water–ethylene glycol (50: 50) hybrid nanofluid using artificial neural network, J. Therm. Anal. Calorim. 143 (2) (2021) 1119–1128.
[23] F. Soltani, D. Toghraie, A. Karimipour, Experimental measurements of thermal conductivity of engine oil-based hybrid and mono nanofluids with tungsten oxide (wo3) and mwcnts inclusions, Powder Technol. 371 (2020) 37–44.
[24] B. Ruhani, P. Barnoon, D. Toghraie, Statistical investigation for developing a new model for rheological behavior of silica–ethylene glycol/water hybrid Newtonian nanofluid using experimental data, Phys. Stat. Mech. Appl. 525 (2019) 616–627.
[25] E. Khodabandeh, S.A. Rozati, M. Joshaghani, O.A. Akbari, S. Akbari, D. Toghraie, Thermal performance improvement in water nanofluid/gnp–sdbs in novel design of double-layer microchannel heat sink with sinusoidal cavities and rectangular ribs, J. Therm. Anal. Calorim. 136 (3) (2019) 1333–1345.
[26] S.-R. Yan, D. Toghraie, L.A. Abdulkareem, A. Alizadeh, P. Barnoon, M. Afrand, The rheological behavior of mwcnts–zno/water–ethylene glycol hybrid non-Newtonian nanofluid by using of an experimental investigation, J. Mater. Res. Technol. 9 (4) (2020) 8401–8406.
[27] I.A. Abro, M.I. Abro, M.E. Assad, M. Rahimi-Gorji, N.M. Hoang, Investigation and evaluation of neem leaves extract as a green inhibitor for corrosion behavior of mild steel: an experimental study, Proc. IME C J. Mech. Eng. Sci. 235 (4) (2021) 734–743.
[28] I.M. Alarifi, V. Movva, M. Rahimi-Gorji, R. Asmatulu, Performance analysis of impact-damaged laminate composite structures for quality assurance, J. Braz. Soc. Mech. Sci. Eng. 41 (8) (2019) 1–16.
[29] R. Asmatulu, K.S. Erukala, M. Shinde, I.M. Alarifi, M.R. Gorji, Investigating the effects of surface treatments on adhesion properties of protective coatings on carbon fiber-reinforced composite laminates, Surf. Coating. Technol. 380 (2019), 125006.
[30] G. Chinni, I.M. Alarifi, M. Rahimi-Gorji, R. Asmatulu, Investigating the effects of process parameters on microalgae growth, lipid extraction, and stable nanoemulsion productions, J. Mol. Liq. 291 (2019), 111308.
[31] S. Kasaragadda, I.M. Alarifi, M. Rahimi-Gorji, R. Asmatulu, Investigating the effects of surface superhydrophobicity on moisture ingression of nanofiber-reinforced bio-composite structures, Microsyst. Technol. 26 (2) (2020) 447–459.
[32] D. Habib, N. Salamat, S. Abdal, I. Siddique, M. Salimi, A. Ahmadian, On time dependent mhd nanofluid dynamics due to enlarging sheet with bioconvection and two thermal boundary conditions, Microfluid. Nanofluidics 26 (2) (2022) 1–15.
[33] S. Abdal, I. Siddique, S. Afzal, S. Sharifi, M. Salimi, A. Ahmadian, An analysis for variable physical properties involved in the nano-biofilm transportation of sutterby fluid across shrinking/stretching surface, Nanomaterials 12 (4) (2022) 599.
[34] B. Ali, S. Hussain, S.I.R. Naqvi, D. Habib, S. Abdal, Aligned magnetic and bioconvection effects on tangent hyperbolic nanofluid flow across faster/slower stretching wedge with activation energy: finite element simulation, Int. J. Algorithm. Comput. Math. 7 (4) (2021) 1–20.
[35] F. Ahmad, S. Abdal, H. Ayed, S. Hussain, S. Salim, A.O. Almatroud, The improved thermal efficiency of maxwell hybrid nanofluid comprising of graphene oxide plus silver/kerosene oil over stretching sheet, Case Stud. Therm. Eng. 27 (2021), 101257.
[36] N. Acharya, F. Mabood, On the hydrothermal features of radiative fe 3 o 4–graphene hybrid nanofluid flow over a slippery bended surface with heat source/sink, J. Therm. Anal. Calorim. 143 (2021) 1273–1289.
[37] I. Tlili, H.A. Nabwey, M.G. Reddy, N. Sandeep, M. Pasupula, Effect of resistive heating on incessantly poignant thin needle in magnetohydrodynamic sakiadis hybrid nanofluid, Ain Shams Eng. J. 12 (1) (2021) 1025–1032.
[38] A. Ali, A. Noreen, S. Saleem, A. Aljohani, M. Awais, Heat transfer analysis of cu–al 2 o 3 hybrid nanofluid with heat flux and viscous dissipation, J. Therm. Anal. Calorim. 143 (3) (2021) 2367–2377.
[39] A.J. Chamkha, R. Yassen, M.A. Ismael, A. Rashad, T. Salah, H.A. Nabwey, Mhd free convection of localized heat source/sink in hybrid nanofluid-filled square cavity, J. Nanofluids 9 (1) (2020) 1–12.
[40] N.C. Roy, I. Pop, Exact solutions of Stokes' second problem for hybrid nanofluid flow with a heat source, Phys. Fluids 33 (6) (2021), 063603.
[41] S. Shehzad, M. Sheikholeslami, T. Ambreen, A. Shafee, H. Babazadeh, M. Ahmad, Heat transfer management of hybrid nanofluid including radiation and magnetic source terms within a porous domain, Appl. Nanosci. 10 (12) (2020) 5351–5359.
[42] K. Ghachem, W. Aich, L. Kolsi, Computational analysis of hybrid nanofluid enhanced heat transfer in cross flow micro heat exchanger with rectangular wavy channels, Case Stud. Therm. Eng. 24 (2021), 100822.
[43] A.U. Yahya, N. Salamat, W.-H. Huang, I. Siddique, S. Abdal, S. Hussain, Thermal characteristics for the flow of williamson hybrid nanofluid (mos2+ zno) based with engine oil over a stretched sheet, Case Stud. Therm. Eng. 26 (2021), 101196.
[44] M.H. Aghahadi, M. Niknejadi, D. Toghraie, An experimental study on the rheological behavior of hybrid tungsten oxide (wo3)-mwcnts/engine oil Newtonian nanofluids, J. Mol. Struct. 1197 (2019) 497–507.
[45] B. Ali, R.A. Naqvi, L. Ali, S. Abdal, S. Hussain, A comparative description on time-dependent rotating magnetic transport of a water base liquid h2o with hybrid nano-materials al2o3-cu and al2o3-tio2 over an extending sheet using buongiorno model: finite element approach, Chin. J. Phys. 70 (2021) 125–139.
[46] N. Iftikhar, A. Rehman, H. Sadaf, Theoretical investigation for convective heat transfer on cu/water nanofluid and (sio2-copper)/water hybrid nanofluid with mhd and nanoparticle shape effects comprising relaxation and contraction phenomenon, Int. Commun. Heat Mass Tran. 120 (2021), 105012.
[47] C. Wang, Free convection on a vertical stretching surface, ZAMM-J. Appl. Math. Mech./Zeitschrift für Angewandte Mathematik und Mechanik 69 (11) (1989) 418–420.
[48] W. Khan, I. Pop, Boundary-layer flow of a nanofluid past a stretching sheet, Int. J. Heat Mass Tran. 53 (11–12) (2010) 2477–2483.